Supplementary Information

Synchronous Monitoring of Underwater Dynamic/Static Pressure Based on Piezoelectric/Capacitive Polyester Elastomer/Carbon Nanotube Composites

Yuxing Tang[a†], *Qing Dang*[a†], *Wei Zhang*[b], *Haiquan Guo*[e], *Hong Pan*[a], *Yong Xiang*[a,d], *Bin Liao*[*, b] *and Xiaoran Hu*[*, a, d]

[a] School of Materials and Energy, University of Electronic Science and Technology of China, Chengdu, China

[b] Key Laboratory of Photochemical Conversion and Optoelectronic Materials, Technical Institute of Physics and Chemistry, Chinese Academy of Sciences, No. 29 Zhongguancun East Road, Haidian District, Beijing 100190, P. R. China

[c] Advanced Energy Institute, University of Electronic Science and Technology of China, Chengdu, China

[d] Sichuan flexible display materials genome engineering center, Chengdu, China

[e] Inner mongolia north hauler joint stock company limited, GHQ@CHINANHL.COM

(Correspondence to Bin Liao, email: binliao@mail.ipc.ac.cn and Xiaoran Hu, e-mail: Huxiaoran@uestc.edu.cn)

[†] Equal contributions

Fig S1 and Fig S2 demonstrate the preparation of DPBPE composite as well as DPBPE sensors, respectively.

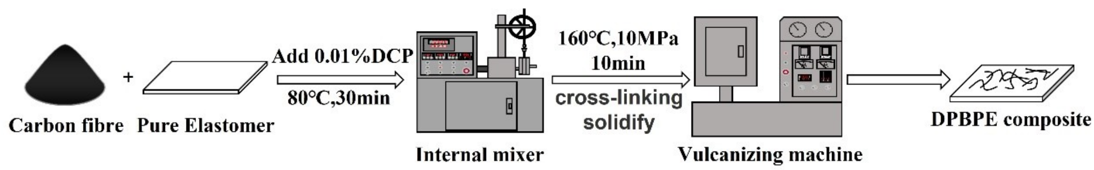

Figure S1. Preparation of DPBPE composite

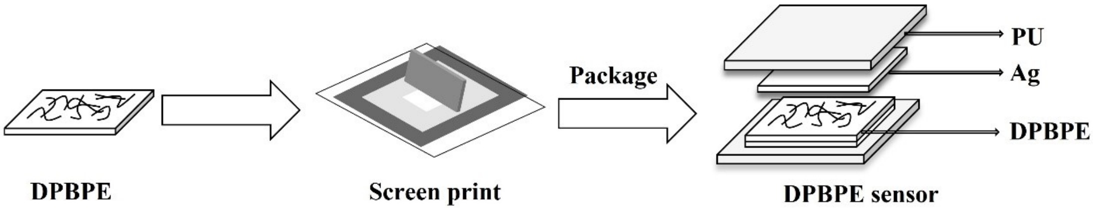

Figure S2. Preparation of DPBPE sensor

The compositions of the DPBPE material are confirmed by ^{1}HNMR in Figure S3. The characteristic peaks at 1.51 ppm (a) and 5.08 ppm (b) are derived from hypo methylene group and side methyl group in lactic acid, respectively. The peaks at 5.73 ppm (c) and 6.35 ppm (d) are peaks for the two protons from C=C in itaconic acid, and the characteristic peak at 3.36 ppm (e) is the proton adjacent to the double bond in itaconic acid. The characteristic peaks at 1.29 ppm (h), 1.62 ppm (g) and 2.29 ppm (f,i) origin from sebacic acid. The peaks at 1.71 ppm (k) and 4.09 ppm (j,l) belong to butane-1,4-diol , and the split peak at 4.09 ppm is due to the different chemical environments around the butane-1,4-diol. The ^{1}HNMR results (Figure S1) confirms the DPBPE material is synthesized with designed chemical compositions.

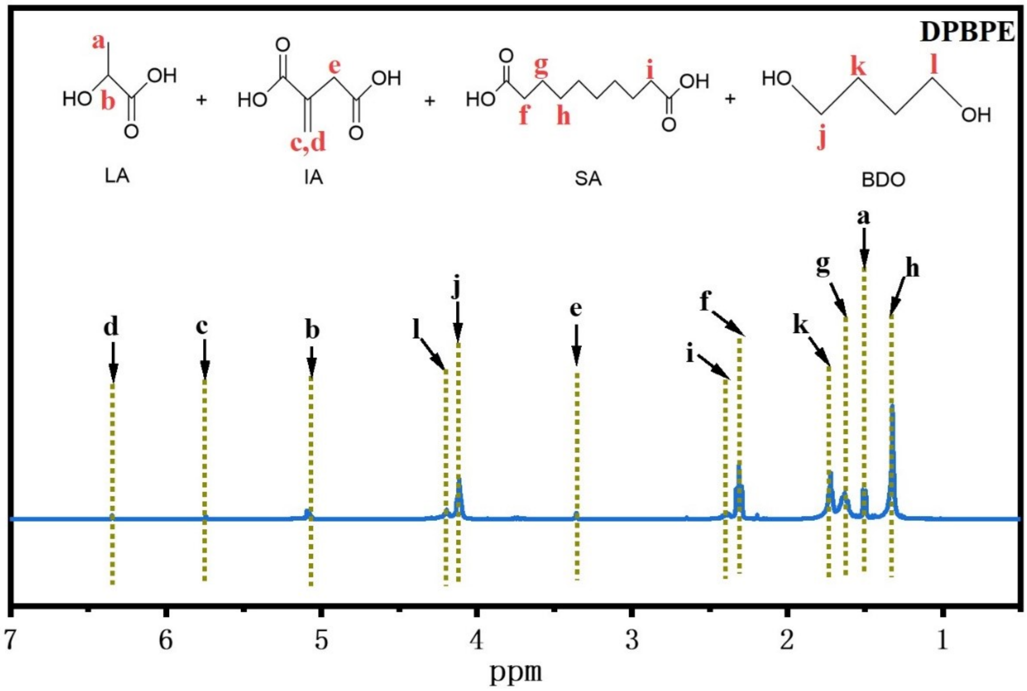

Figure S3. [1]H-MR spectra of the DPBPE material

In Figure S4, when a high pressure of 54 kPa is applied on the DPBPE sensor, its internal dipoles deflections, generating a piezoelectric current of 12 nA. Once stabilized, the distance between internal carbon fibers decreases with the applied pressure, resulting in a change in capacitance value. When an extra pressure as low as 9.8Pa is applied while the high pressure of 54kPa exists, a piezoelectric signal is still capable to be observed indicating its piezoelectric and captative function serves without any mutual interference.

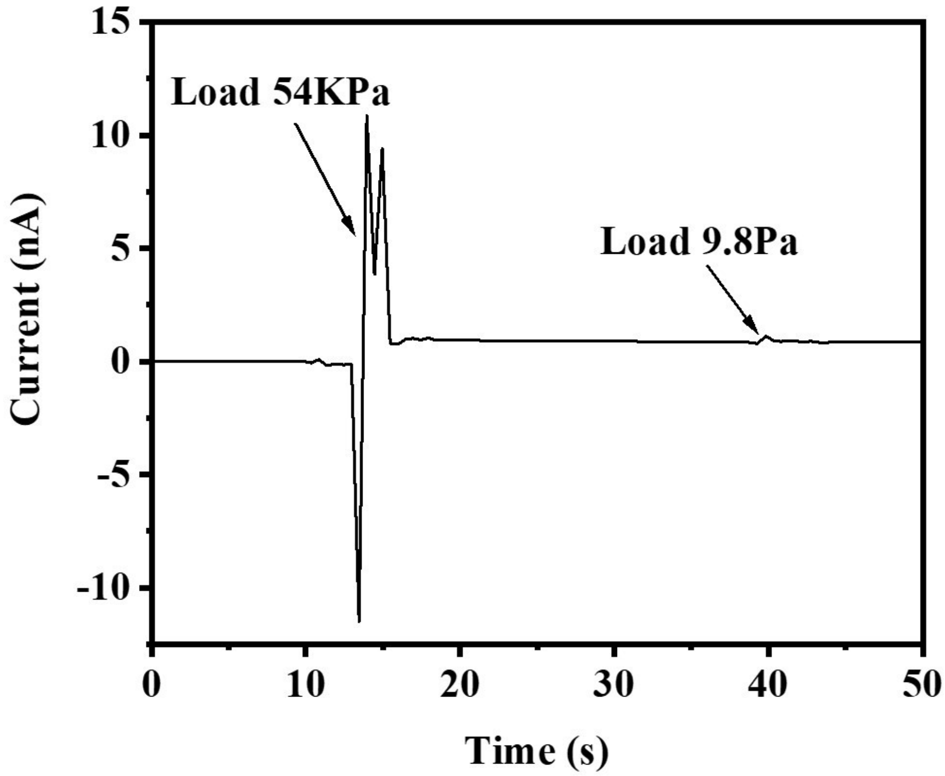

Figure S4. Applying a feedback of 9.8 Pa at a high pressure of 54 kPa.

Table S1 shows the performance of the sensors in different materials and constructions. Compared to these the DPBPE sensors have the advantage of achieving integrated and synchronous identification of dynamic and static pressures as well as a wide measuring range.

Table S1 Performance comparison of different sensors

Materials	**Framework**	**Measurement range**	**Static pressure sensitivity**	**Dynamic pressure sensitivity**	**Simultaneous identification**
DPBPE	--	250 kPa	0.031 kPa^{-1}	0.8 mV/N	⚐
Mxene/LS/PVA[1]	Fiber film	250 kPa	5.5 kPa^{-1}	low	--

Perfluorocarbon/PDMS[2]	Hierarchically porous	400 kPa	0.18 kPa^{-1}	low	--
PVDF-TrFE/Mxene[3]	Fiber film	20N	--	2.51mV/(N*μm)	--
PDMS/PVDF[4]	Multilayer architecture	800 kPa	--	7.7 mV/kPa	--
PVDF/PVDF-TrFE[5]	Nanopillars	80N	--	250mV/N	--

In Fig. S5 the capacitance values fed back by the step pressure are shown, with the steps becoming less pronounced as the pressure value increases, reaching the upper measurement limit at 240 kPa.

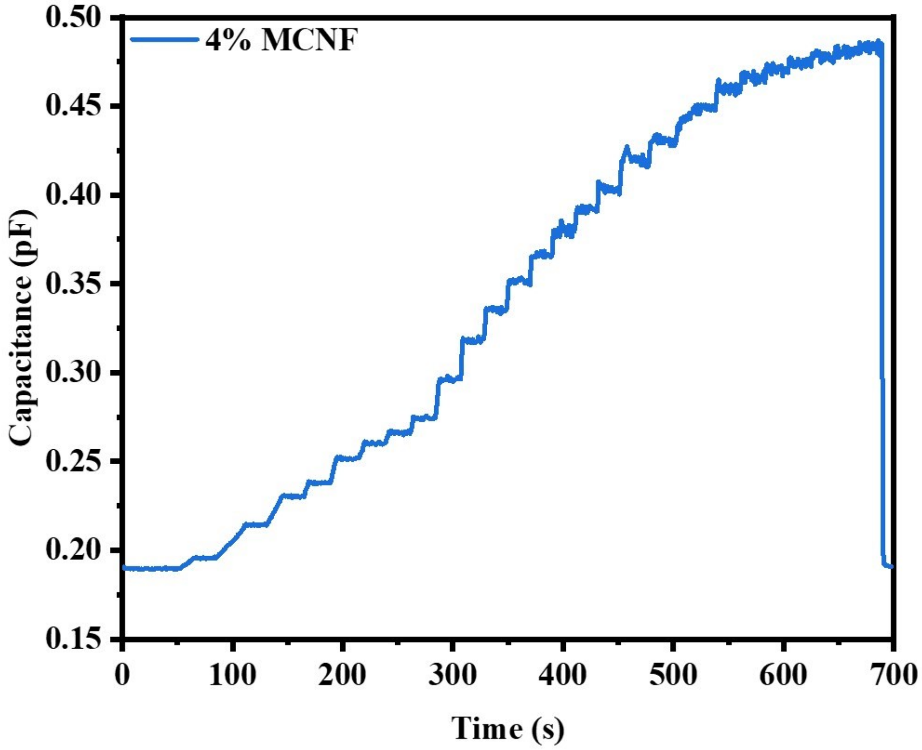

Figure S5. Capacitance value corresponding to the step pressure from 0 to 240kpa

In Fig. S6, when the DPBPE sensor is subjected with higher pressure, the internal micro-capacitor plate spacing is further reduced and the dipole deflection is increased, presenting higher capacitance and voltage values.

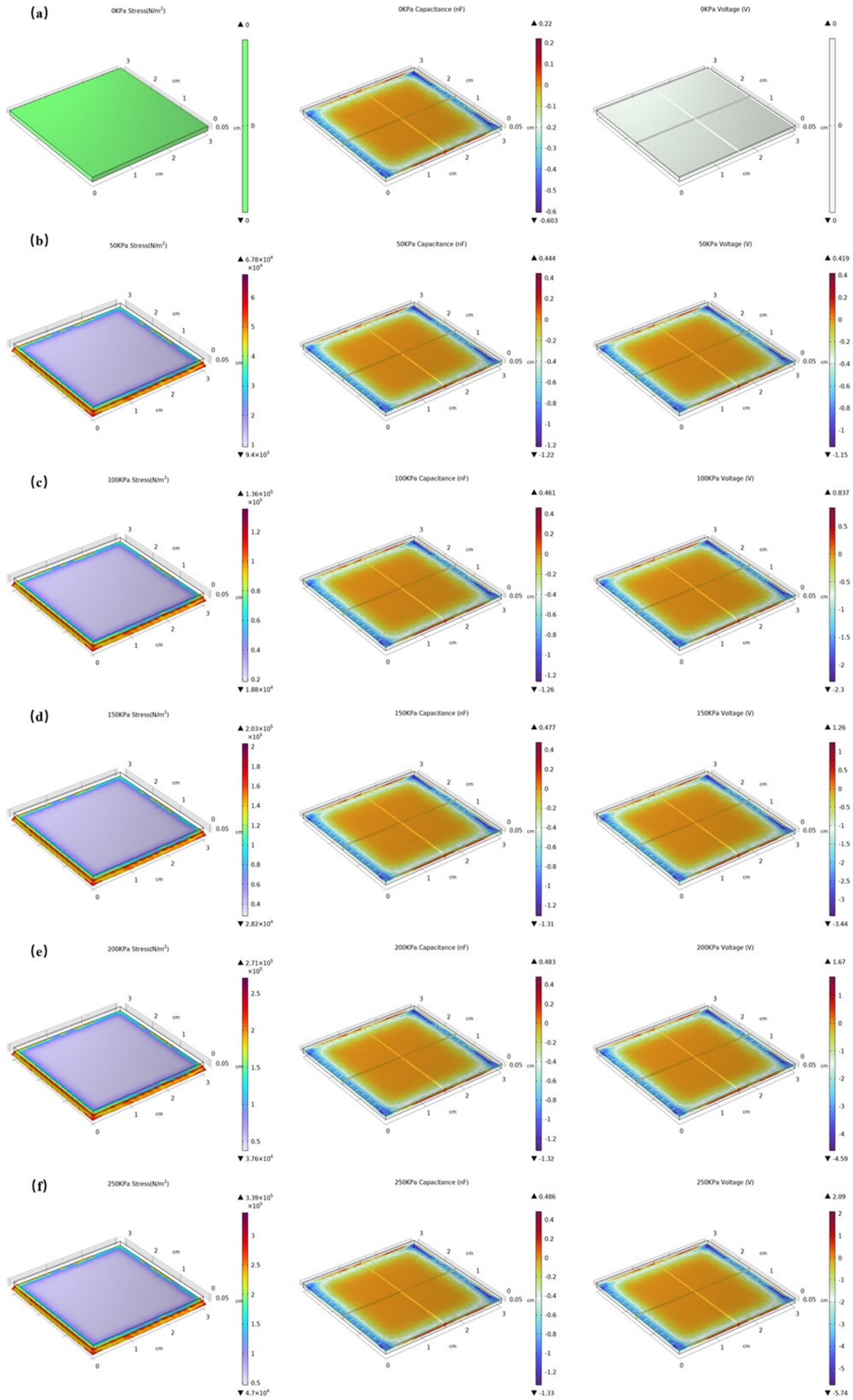

Figure S6 The deformation, capacitance and voltage response of DPBPE under different pressures. (a)0 kPa, (b)50 kPa, (c)100 kPa, (d)150 kPa, (e)200 kPa, (f)250kPa.

In Fig. S7, the 4% MCNF DPBPE exhibits a higher C peak and a lower O peak, compared to blank DPBPE. This is due to the interface interaction between the elastomer and MCNF.

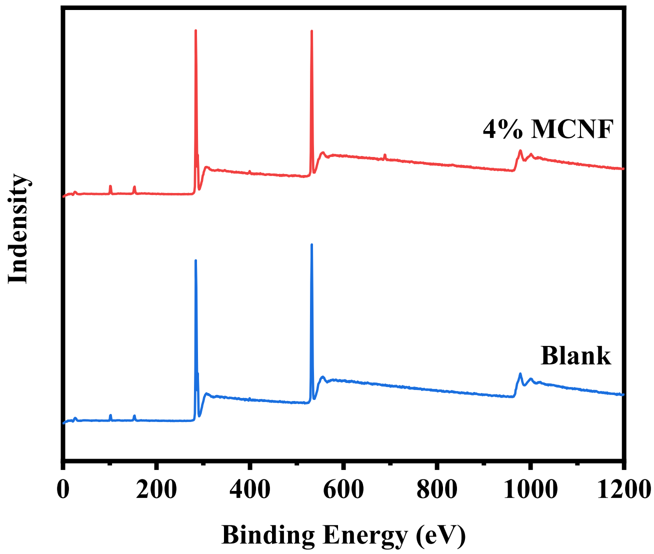

Figure S7. XPS of 4%MCNF and Blank DPBPE

Table S2 Performance comparison of capacitance sensors

Materials	range	respose to small forces	Relative Capacitance Change Rate	Sensitivity	Response Time	Recovery Time
DPBPE	0-240 kpa	⚐ (1 kpa)	154%	3.09×10-2 kPa-1	75 ms	100ms
Ga-In/PDMS[6]	0-1.10 MPa	-	13.1%	11 kPa-1	-	-
CB/PDMS[7]	0–20 N	⚐ (0.1 N)	90.4%	0.028N−1	-	-
CB/PDMS[8]	0-320kpa	-	4.30%	-	-	-
PDMS[9]	0-111kpa	⚐ (0.2 Pa)	152%	0.078 Pa-1	100ms	100ms

CNTs/PDMS[10]	0-10kpa	⚐（~100 Pa）	~70%	0.1980 kPa−1	<200ms	-

In Fig. S8, compared to neat DPBPE, the glass transition temperature of 4% MCNF/DPBPE composite material did not show a significant increase. Additionally, the composite material maintained its amorphous structure during the cooling process, which indicates that the 4% MCNF/DPBPE composite maintains a high elasticity and amorphous structure at temperatures above -50°C.

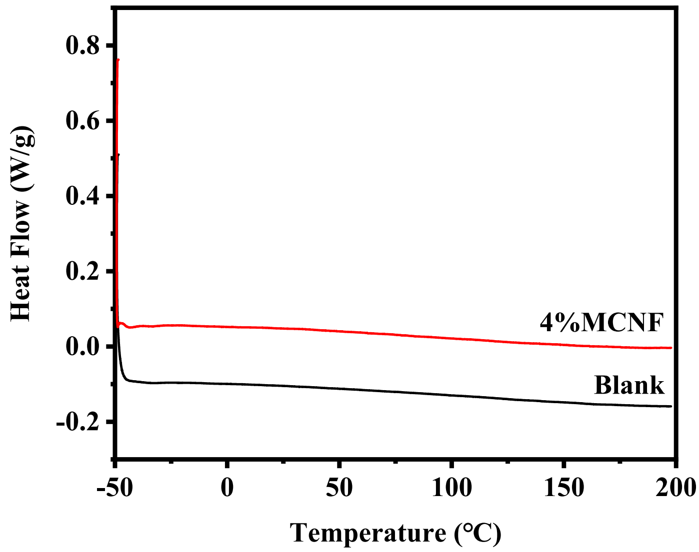

Figure S8. DSC of 4%MCNF and Blank DPBPE

Reference

1. S. Sharma, A. Chhetry, S. Zhang, H. Yoon, C. Park, H. Kim, M. Sharifuzzaman, X. Hui and J. Y. Park, *ACS Nano*, 2021, **15**, 4380-4393.
2. J. Hwang, Y. Kim, H. Yang and J. H. Oh, *Composites Part B: Engineering*, 2021, **211**.
3. S. Wang, H.-Q. Shao, Y. Liu, C.-Y. Tang, X. Zhao, K. Ke, R.-Y. Bao, M.-B. Yang and W. Yang, *Composites Science and Technology*, 2021, **202**.
4. W. Lin, B. Wang, G. Peng, Y. Shan, H. Hu and Z. Yang, *Advanced Science*, 2021, **8**.
5. R. A. Surmenev, R. V. Chernozem, I. O. Pariy and M. A. Surmeneva, *Nano Energy*, 2021, **79**.
6. S. Ali, D. Maddipatla, B. B. Narakathu, A. A. Chlaihawi, S. Emamian, F. Janabi, B. J. Bazuin and M. Z. Atashbar, *IEEE Sensors Journal*, 2019, **19**, 97-104.
7. Y. Zhu, X. Chen, K. Chu, X. Wang, Z. Hu and H. Su, *Sensors*, 2022, **22**, 628.

8. Y. Ko, H. Yoon, S. Kwon, H. Lee, M. Park, I. Jeon, J. A. Lim, S. Chung, S.-S. Lee, B. J. Sung, J.-H. Kim and H. Kim, *Composites Part B: Engineering*, 2020, **201**, 108337.
9. Bijender and K. Ashok, *Materials Chemistry and Physics*, 2023, **304**, 127872.
10. J. Cui, B. Zhang, J. Duan, H. Guo and J. Tang, *Journal*, 2016, **16**.